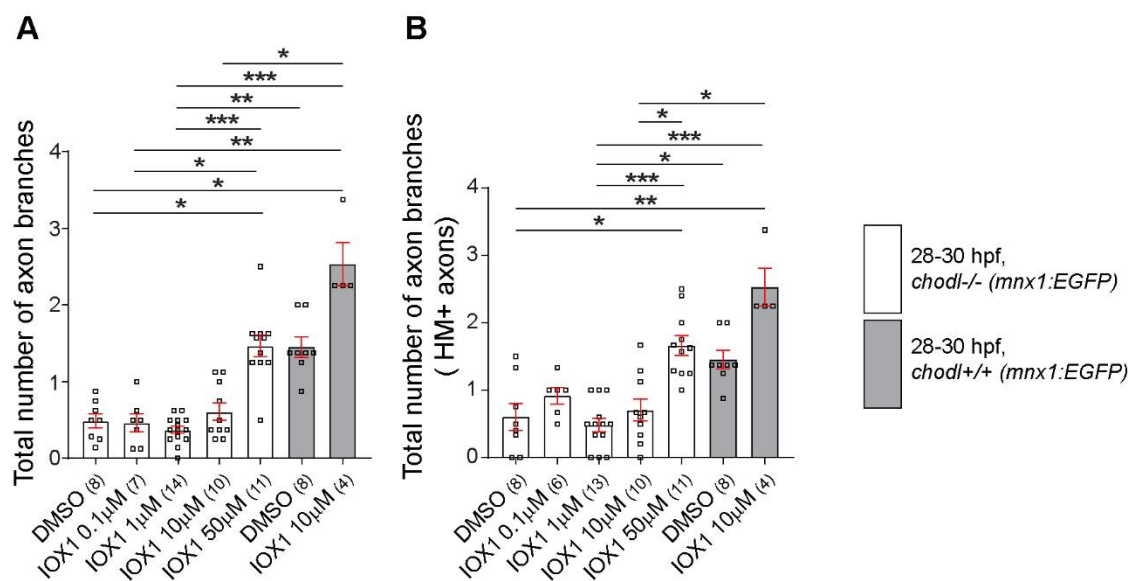


**Figure S1: Drug/small molecules from the initial screening that rescue the growth of CaP motor neurons in *chodl* mutant and do not affect the development of the embryos.** (A) The percentage of CaP motor axons that pass the horizontal myospetum is shown. Each group is presented in relation to its own DMSO-control (gray bars) preceding each group of drugs. These data relate to Fig. 2B. (B) Representative images of 28-29 hpf embryos (lateral view) after the first screening are shown. Black arrow heads indicate CaP motor axons that passed

beyond the horizontal myoseptum (solid yellow line). Scale bar: 50  $\mu\text{m}$ . (C) Quantification of the length from the dorsal edge of the trunk to the ventral edge of the embryos is shown. No significant differences were observed between DMSO- and drug-treated mutants [Kruskal-Wallis test ( $p = 0.0212$ ) with Dunn's multiple comparison test - no significant differences detected]. (D) Representative images of 28-29 hpf *chodl* embryos that pass through the VAST capillary for imaging are shown. Scale bar: 300  $\mu\text{m}$ .

Each data point represents one animal. N-numbers are indicated in each bar. Error bars represent means  $\pm$  SEM.



**Figure S2: Axonal branching analysis for IOX1-treated *chodl* mutants. (A)**

Quantification of axonal branching is shown. 50  $\mu$ M IOX1 induced an increase in the total number of axonal branches, reaching control-levels (Kruskal-Wallis test \*\*\*\* $p < 0.0001$  with Dunn's multiple comparison test: DMSO-*chodl* mutant vs 50  $\mu$ M-*chodl* mutant \* $p = 0.0380$ , DMSO-*chodl* mutant vs IOX1 10 $\mu$ M-control \* $p = 0.0131$ , IOX1 0.1  $\mu$ M-*chodl* mutant vs IOX1 50  $\mu$ M-*chodl* mutant \* $p = 0.0270$ , IOX1 0.1  $\mu$ M-*chodl* mutant vs IOX1 10 $\mu$ M-control \*\* $p = 0.0093$ , IOX1 1  $\mu$ M-*chodl* mutant vs 50  $\mu$ M-*chodl* mutant \*\*\* $p = 0.0004$ , IOX1 1  $\mu$ M-*chodl* mutant vs DMSO-control \*\* $p = 0.0021$ , IOX1 1  $\mu$ M-*chodl* mutant vs IOX1 10 $\mu$ M-control \*\*\* $p = 0.0006$ , IOX1 10  $\mu$ M-*chodl* mutant vs IOX1 10 $\mu$ M-control \* $p = 0.0181$ , 50  $\mu$ M-*chodl* mutant vs DMSO-control  $p > 0.9999$ , 50  $\mu$ M-*chodl* mutant vs IOX1 10 $\mu$ M-control  $p > 0.9999$ , DMSO-control vs IOX1 10 $\mu$ M-control  $p > 0.9999$ , statistical power = 1.00). (B) Quantification of axonal branches for CaP axons that passed the horizontal myoseptum is shown. IOX1 increases the number of branches in *chodl* mutants (Kruskal-Wallis test \*\*\*\* $p < 0.0001$  with Dunn's multiple comparison test: DMSO-*chodl* mutant vs 50  $\mu$ M-*chodl* mutant \* $p = 0.0223$ , DMSO-*chodl* mutant vs IOX1 10 $\mu$ M-control \*\* $p = 0.0092$ , IOX1 1  $\mu$ M-*chodl* mutant vs 50  $\mu$ M-*chodl* mutant \*\*\* $p = 0.0005$ , IOX1 1  $\mu$ M-*chodl* mutant vs DMSO-control \* $p = 0.0115$ , IOX1 1  $\mu$ M-*chodl* mutant vs IOX1 10 $\mu$ M-control \*\*\* $p = 0.0007$ , IOX1 10  $\mu$ M-*chodl* mutant vs IOX1 50  $\mu$ M-*chodl* mutant \* $p = 0.0414$ , IOX1 10  $\mu$ M-*chodl* mutant vs IOX1 10 $\mu$ M-control \* $p = 0.0168$ , 50  $\mu$ M-*chodl* mutant vs DMSO-control  $p > 0.9999$ , 50  $\mu$ M-*chodl* mutant vs IOX1 10 $\mu$ M-control  $p > 0.9999$ , DMSO-control vs IOX1 10 $\mu$ M-control  $p > 0.9999$ , statistical power = 1.00).

Each data point represents one animal. N-numbers are indicated in brackets under each bar. Error bars represent means  $\pm$  SEM.

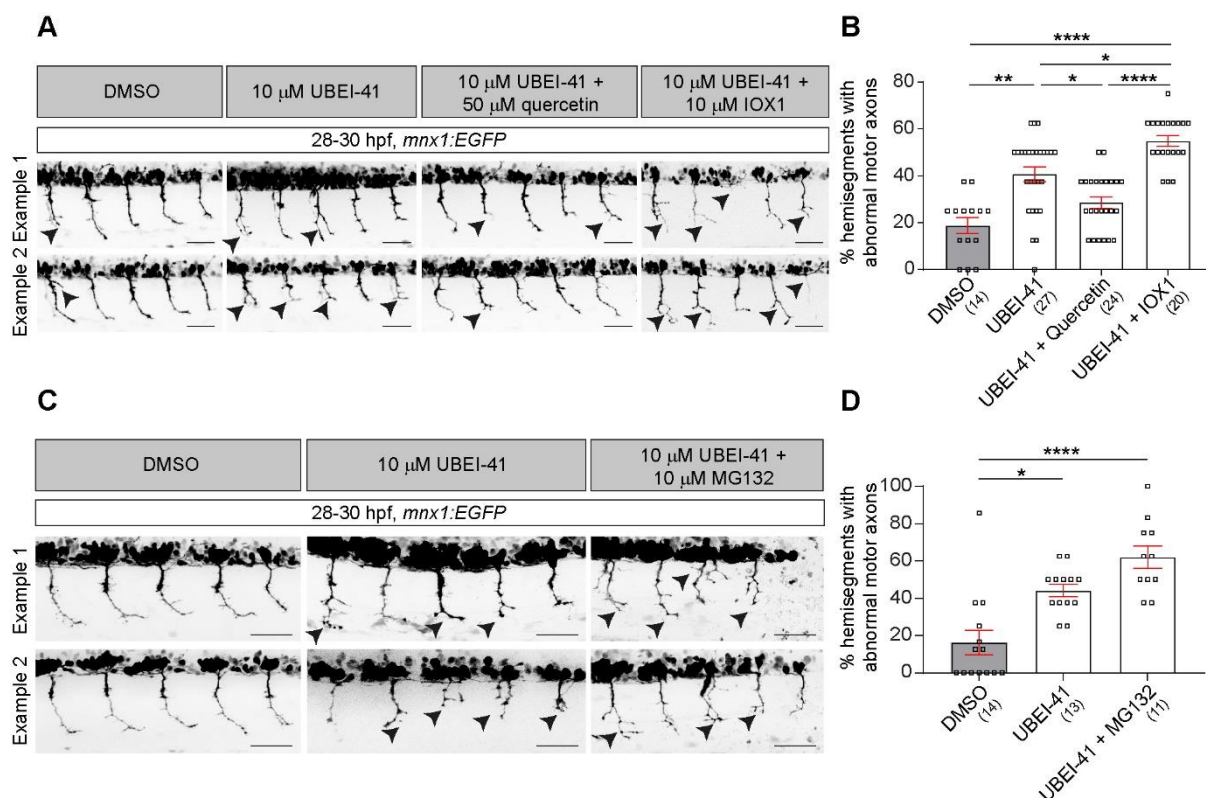
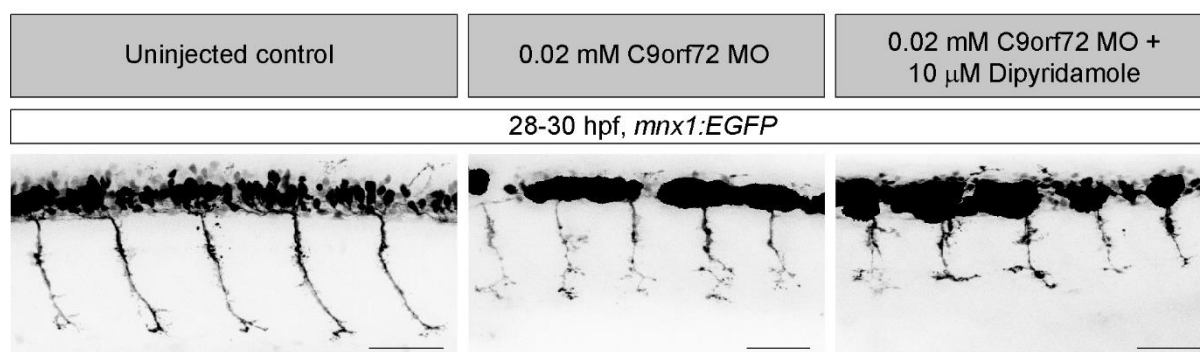


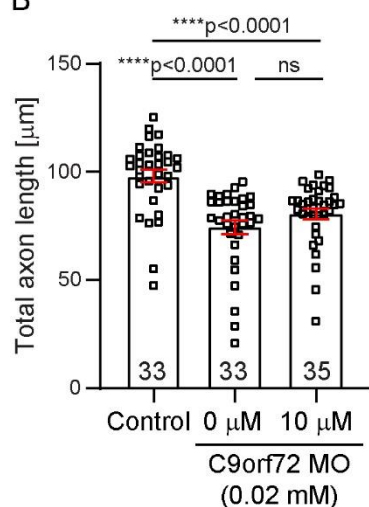
**Figure S3: Axonal abnormal morphology of the UBEI-41 model are not rescued by IOX1 or MG132.** (A) Representative images (lateral view) of 28-30 hpf drug treated *mnx1:EGFP* embryos (lateral view) are shown: DMSO (vehicle), UBEI-41 (SMA-like phenotype), UBEI-41+ quercetin (internal positive rescue control) and UBEI-41 + IOX1 (experimental condition). (B) The positive control quercetin rescues motor axon morphology induced by UBEI-41 (Kruskal-Wallis test \*\*\*\* $p < 0.0001$  with Dunn's Multiple Comparison Test: UBEI-41 vs UBEI-41 + quercetin \* $p = 0.474$ ), but IOX1 treatment does not (DMSO vs UBEI-41 \*\* $p = 0.0013$ , DMSO vs UBEI-41 + IOX1 \*\*\*\* $p < 0.0001$ , UBEI-41 vs UBEI-41 + IOX1 \* $p = 0.0441$ ). Statistical power for the whole statistical analysis = 0.999. (C) Representative images (lateral view) of 28-30 hpf drug treated *mnx1:EGFP* embryos (lateral view) are shown. (D) Quantification of the abnormal motor axons after MG132 treatment is shown (Kruskal-Wallis test \*\*\*\* $p < 0.0001$  with Dunn's multiple comparison test: \*\*\*\* $p < 0.0001$ , \* $p = 0.0139$ , statistical power = 0.999).

All the examples of abnormal motor neurons are indicated by black arrowheads. All scale bar: 50  $\mu$ m. Each data point represents one animal. N-numbers are indicated in brackets under each bar. Error bars represent means  $\pm$  SEM.

**A**



**B**



**C**

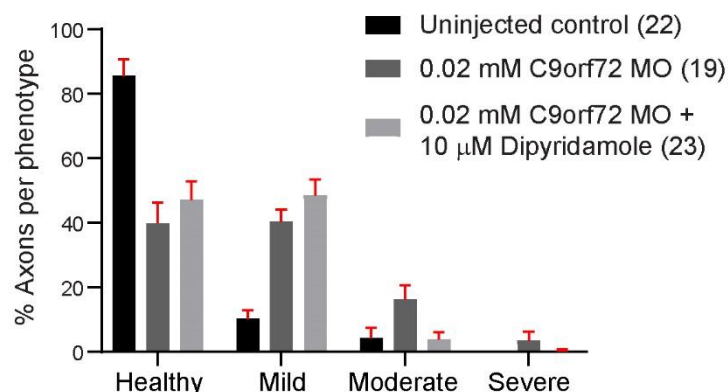


**Figure S4: Dipyridamole treatment of C9orf72 knockdown zebrafish does not rescue the phenotype.** (A) Micrographs of example axons from uninjected controls compared to C9orf72 knockdown without and with 10  $\mu$ M dipyridamole, respectively. Scale bar: 50  $\mu$ m. (B) Axon length analysis of C9orf72 knockdown zebrafish treated with dipyridamole. There is no significant difference between axon lengths of dipyridamole-treated zebrafish compared to C9orf72 knockdown alone (Kruskal-Wallis test \*\*\*\* $p < 0.0001$  with Dunn's multiple comparison test, statistical significance power = 0.9998). Each point represents the average axon length of one fish (12 axons per fish). (C) There is no significant difference in axon phenotypes between dipyridamole-treated zebrafish compared to C9orf72 knockdown alone in any category (two-way ANOVA,  $p < 0.0001$ ,  $F(6,244) = 23.96$ , with Tukey's multiple comparison test, C9orf72 MO vs C9orf72 MO + dipyridamole, 'healthy'  $p = 0.3972$ ; 'mild'  $p = 0.3017$ ; 'moderate'  $p = 0.0712$ ; 'severe'  $p = 0.8370$ ). N-numbers are indicated in each bar. Error bars represent means  $\pm$  SEM.